Supplement of Atmos. Chem. Phys., 15, 10669–10685, 2015
http://www.atmos-chem-phys.net/15/10669/2015/
doi:10.5194/acp-15-10669-2015-supplement

Atmospheric Chemistry and Physics Open Access

Supplement of

Influence of crustal dust and sea spray supermicron particle concentrations and acidity on inorganic NO_3^- aerosol during the 2013 Southern Oxidant and Aerosol Study

H. M. Allen et al.

Correspondence to: J. L. Fry (fry@reed.edu)

1 Emissions sources

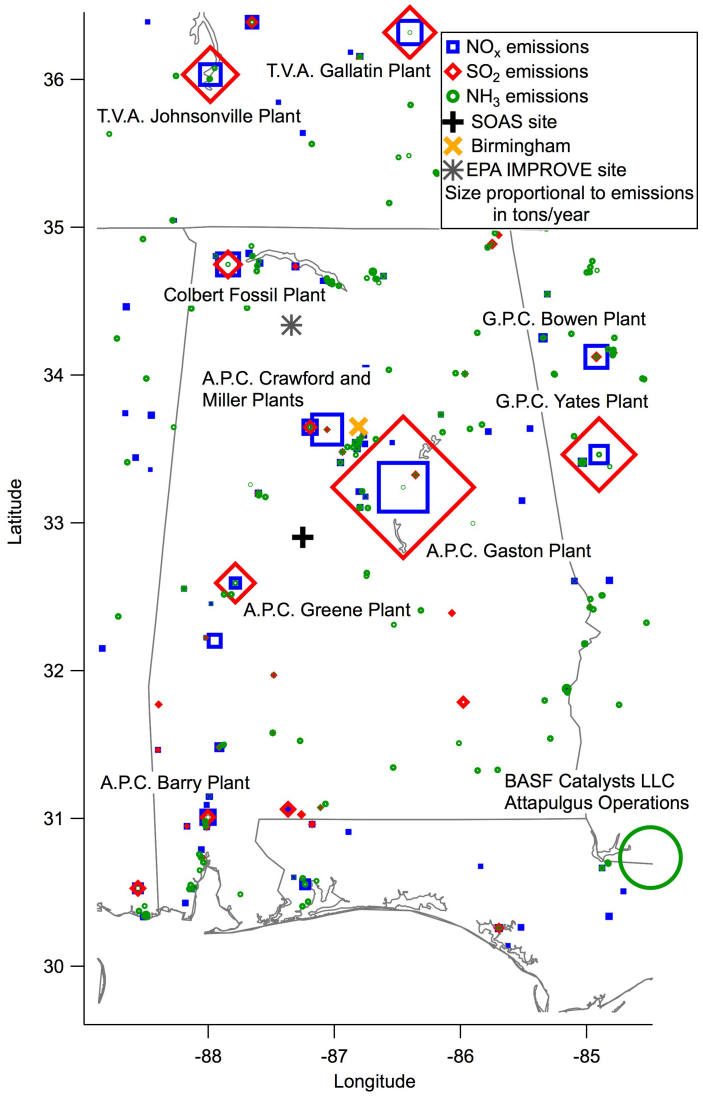

Figure S1: Point sources of SO_2, NO_x, and NH_3 in and around Alabama. Major pollution point sources include various electric generating plants primarily operated by the Alabama Power Company (APC), which emits 91,735 tons SO_2 per year and 16,982 tons NO_x per year (Ernest C. Gaston plant), and the BASF Catalysists LLC - Attapulgus Operations, a mineral processing plant, that emits 1,946 tons NH_3 per year. The size of markers is proportional to emissions in tons per year, with NH_3 emissions multiplied by a factor of 10 relative to NO_x and 20 relative to SO_2 for visual clarity.

The SOAS campaign site, located in central Alabama, is influenced by a number of anthropogenic emissions sources (see Figure S1). These sources include the city of Birmingham, AL located 71 km northeast of the site, and numerous coal-fired power plants owned by the Alabama Power Company (APC) located within a 50-mile radius of the sampling site. These power plants include the Ernest C. Gaston plant 45 miles northeast of the site, the William Crawford Gorgas and James H. Miller Jr. plants both 50 miles north of the site, and the Greene County plant 50 miles southwest of the site. Pollution sources and emissions obtained from the 2011 EPA National Emissions Inventory (http://www.epa.gov/ttnchie1/net/2011inventory.html). Regional mobile on-road and off-road sources (not pictured) will also contribute significantly to NO_x concentrations at the site.

2 Temperature and relative humidity

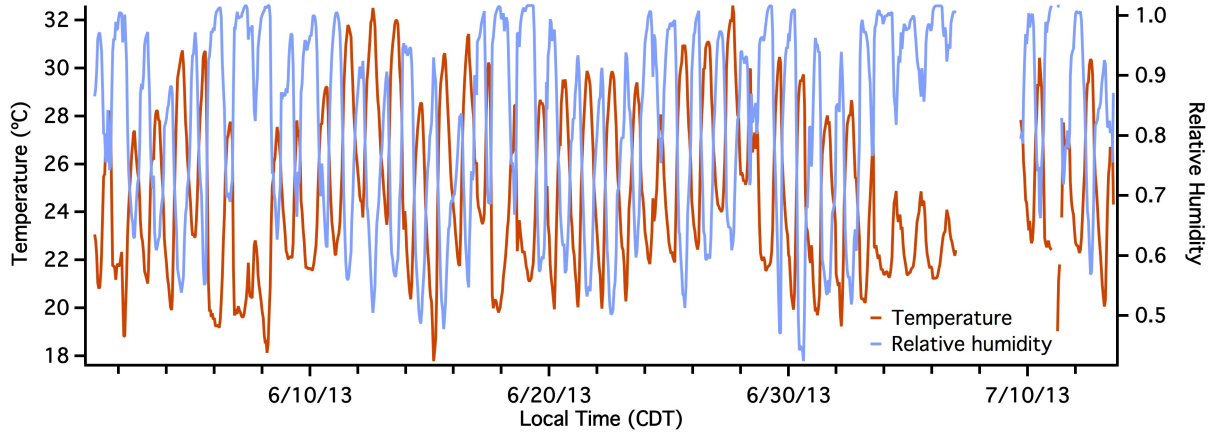

Figure S2: Time series of temperature and RH measured during the 2013 SOAS campaign. Temperature and RH measurements were collected at 1 minute time resolution from the ARA SEARCH monitoring site collocated with the MARGA instrument at the SOAs ground site. The data has been averaged to 1 hour resolution to match MARGA sampling frequency.

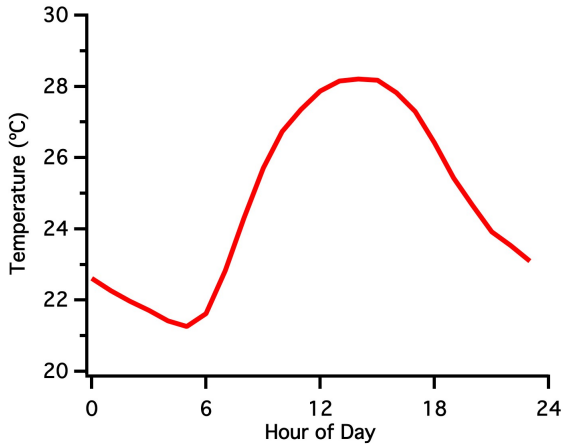

Figure S3: Diurnal profile of measured temperature (°C) at the Centreville measurement site during the 2013 SOAS campaign compared.

While sources may vary over the diurnal cycle and thus different total HNO_3+NO_3^- may be observed, one possible reason for the enhanced HNO_3 observed in the thermodynamic models may be the temperature-driven increases in particle-to-gas conversion. To assess this potential correspondence between temperature and phase partitioning, the diurnal profiles of temperature and HNO_3 were compared (Figure 7 and Figure S3). As expected, semi-volatile HNO_3 generally increases with increasing temperature during the daytime. However, particularly notable is the comparison of this diurnal cycle to that of HNO_3 and NO_3^- predicted by E-AIM. If temperature dependence of phase partitioning were the primary driver of HNO_3 variability, HNO_3 would increase and particulate NO_3^- would decrease by approximately equal amounts on a molar basis during the daytime. While neither of the diurnal profiles from MARGA measurements or from ISORROPIA predictions exhibits this pattern, the diurnal profile of HNO_3 and NO_3^- predicted by E-AIM does.

3 HNO_3 and NO_3^- measurements

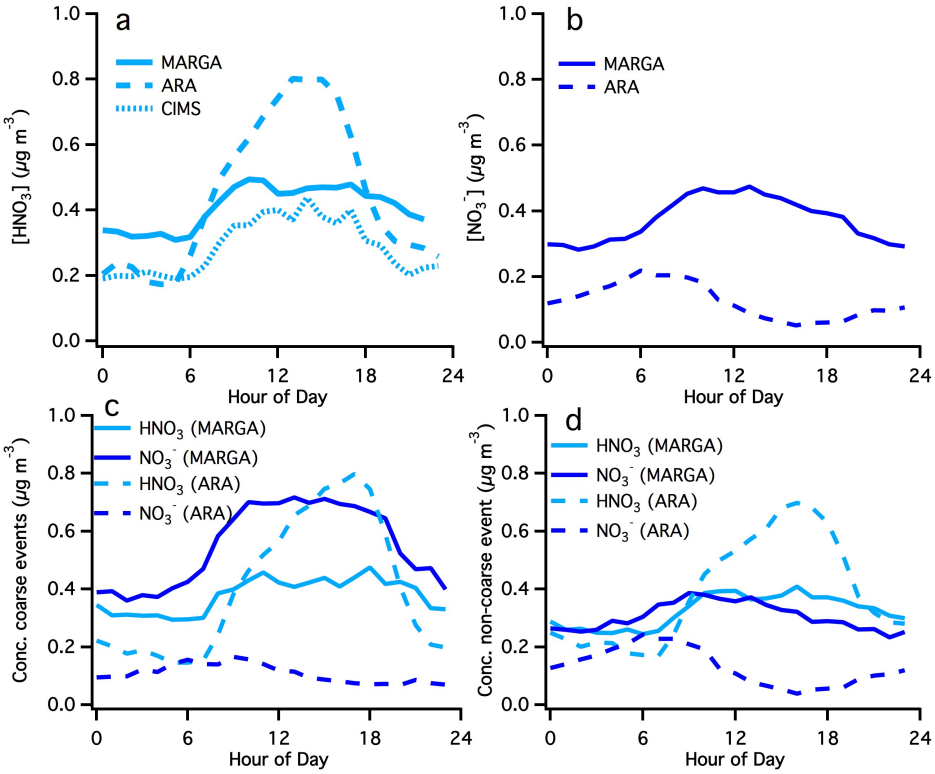

Figure S4: Diurnal profiles of gas phase HNO_3 and aerosol NO_3^- from 3 separate, collocated measurements. (a) HNO_3 from MARGA, ARA, and CIMS measurements averaged between 14 June and 3 July, 2013; (b) NO_3^- from MARGA and ARA measurements, averaged between 1 June and 13 July, 2013; (c) MARGA and ARA measurements averaged during the two coarse particle events; and (d) MARGA and ARA measurements during non-coarse particle days.

To check the robustness of the MARGA measurements of HNO_3, the MARGA measurements are compared to those available from two instruments collocated at the SOAS ground site at Centreville: a denuder-difference measurement made by Atmospheric Research and Analysis, Inc. (ARA) and a Chemical Ionization Mass Spectrometer (CIMS) made by the Wennberg group from the California Institute of Technology. The ARA instrument utilizes an inlet situated 5 m above ground level, with a flow rate of 1.25 L min^{-1}, residence time of less than 2 seconds, and sampling resolution of 1 minute. The instrument measures NO_3^- by difference in NO_y signal from a filtered versus unfiltered channel. Sample air in channel 1 (CH1) passes through a KCl-impregnated HEPA filter, then through a commercial molybdenum (Mo) mesh catalyst heated to 350 °C. The CH1 signal represents the measurement baseline for the analyzer, i.e., instrument dark current and any residual gas-phase NO_y not removed by the inlet lines and filter. Channel 2 (CH2) flows through a KCl-impregnated annular denuder (citric acid) into a parallel Mo converter also heated to 350 °C. The signal from CH2 includes baseline NO_y plus particulate nitrogen species that are convertible to NO. Because 350 °C Mo is essentially blind to reduced nitrogen (ammonia and particulate ammonium), this measurement assumes that nitrate is the only species of consequence (other than baseline NO_y) in the CH2 signal. HNO_3 is similarly measured by denuder difference (using 1% sodium carbonate solution as denuder wall coating), employing a Mo reduction converter and chemiluminescence (Edgerton et al., 2005).

The CIMS instrument is described in detail in Nguyen et al., 2014. Briefly, the instrument was located on the topmost platform of a metal walk-up sampling tower approximately 20 m in height (measurement height was approximately 22 m above ground). The CIMS employed a high-flow fluoropolymer-coated glass inlet (approximately 40 cm long, 3.1 cm ID) with a flow rate of 2,000 L min^{-1}. The analytical method utilizes a CF_3O^- reagent ion, calibrated for absolute sensitivity and water vapor dependence of ionization.

The CIMS reports data as 5 second averages.

As indicated by a diurnal profile of HNO_3 measurements over the campaign timeframe, the three instruments measure slightly different concentrations of HNO_3 relative to each other. A substantially higher daytime HNO_3 peak exists in the ARA measurements compared to the MARGA measurement (Figure S4a). This discrepancy may be caused by a damping of the diurnal cycle of HNO_3 by MARGA from passivation of the TFE lines due to the relatively long residence time (4.4 s compared with less than 2 s for the ARA instrument) of the inlet line (Neuman et al., 1999). However, a third measurement by the CIMS, with a residence time of approximately 0.01 s, does not indicate a strong daytime HNO_3 peak but instead exhibits a diurnal profile more like that of the MARGA. This instrument was located at a substantially higher elevation than the MARGA inlet, and therefore might not be a direct comparison of HNO_3 concentrations, but indicates that dampening of the HNO_3 signal by the long MARGA inlet line does not fully explain the difference between the MARGA and ARA measurements. In addition, the ISORROPIA thermodynamic model (Figure 7c, main text) predicts comparable magnitudes of NO_3^- and HNO_3 mass loadings to the MARGA during the day at the measured temperature and RH conditions of SOAS.

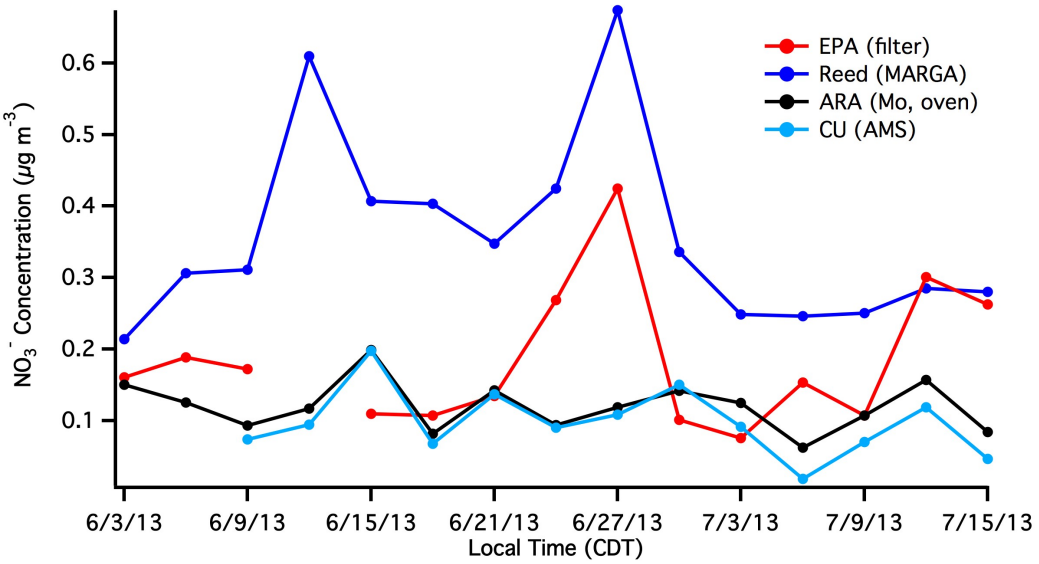

Figure S5: Comparison of NO_3^- measurements from four instruments sampling during the 2013 SOAS campaign. The MARGA, the EPA's filter pack, and ARA's denuder difference measurement all sample with a $PM_{2.5}$ size cut while the AMS samples with a PM_1 size cut. All measurements have been averaged down to a 3-day period to match the EPA time fequency. The difference in these measurements shows evidence that the MARGA size cut may be larger than ARA and thus include more coarse mode NO_3^-. This analysis is consistent with the ambient size distribution during coarse particle events peaking near 3 μm in particle diameter (Figure S7), and with a laboratory test of the $PM_{2.5}$ cyclone used at SOAS showing that a non-negligible fraction of 3 to 5 μm diameter particles penetrate the cyclone at flow rates used in the field.

Similarly, to determine the effect of size cut on NO_3^- measurements, the MARGA is compared to similar measurements by three instruments sampling during the 2013 SOAS campaign: a denuder-difference measurement made by ARA, the EPA's routine filter-pack measurement, and an Aerosol Mass Spectrometer (AMS) operated by the University of Colorado, Boulder. The EPA was collected as part of the Interagency Monitoring of Protected Visual Environments (IMPROVE) particulate monitoring network. The site is located approximately 100 km north of the SOAS sampling site (Fig S1). The NO_3^- measurement is described in detail in Malm, et al., 1994. Briefly, NO_3^- is sampled through a PM2.5 cyclone with a flow rate of 22.7 L min^{-1}. The sample passes through a gas denuder consisting of a set of concentric cylindrical aluminum sheets coated with potassium carbonate to remove HNO_3 before collection. The samples are then collected on a 25-mm Nylon filter, extracted using 23 mL of Dionex IC eluenct in Wheaton low K glass scintillation

vials, and analyzed using ion chromatography. Daily samples are then reported as 3-day averages. The AMS trace shown is from a high-resolution time-of-flight aerosol mass spectrometer (AMS, DeCarlo et al., 2006), with NO_3^- mass loading determined by separation of the total NO_3 signal into inorganic and organic nitrate, as described in Fry et al., 2013.

During the campaign, the MARGA measured higher aerosol NO_3^- loading than similar measurements by the other instruments (Figure S5). The diurnal profile of the MARGA measurements indicates a pronounced midday NO_3^- peak; by contrast, ARA measurements indicate highest NO_3^- concentrations in the early morning (Fig S4b). A comparison of diurnal averages for NO_3^- made by MARGA and the ARA instrument during coarse particle and non-coarse particle events indicates that the MARGA measures substantially higher NO_3^- during the coarse-particle events (Figure S4c and d). On average, the EPA also measured higher NO_3^- than ARA, although lower than the MARGA (Figure S5), yet the distance between the two instruments (approximately 100 km) means the reported concentrations cannot be compared directly. However, the EPA measurement does indicate high NO_3^- aerosol loading during the second coarse particle event identified by the MARGA, suggesting that this coarse mode particle event was regional in scope. In addition, the ARA NO_3^- measurement is more similar to that of the AMS, which employed a PM_1 size cut. Relative to the MARGA, the AMS measured substantially lower concentrations of NO_3^- and the two instruments diverge most prominantly during periods of high aerosol surface area (Figure S6). This comparison indicates the prevalence of supermicron NO_3^- at the SOAS site and suggests that intercomparisons of NO_3^- measurements must take aerosol size into account.

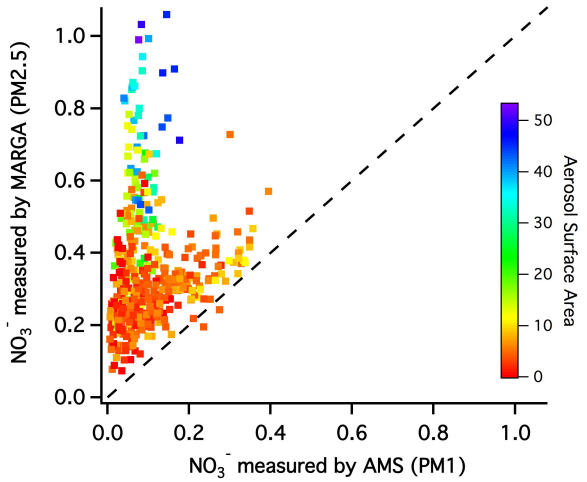

Figure S6: Correlation between NO_3^- measurements made by MARGA and those made by the AMS, colored by the estimated aerosol surface area. The MARGA samples with a $PM_{2.5}$ size cut while the AMS sampled with a PM_1 cut. The instruments diverge most strongly during periods of high aerosol surface area.

The discrepancy between the NO_3^- measurements may arise from the MARGA size cut being higher than the nominal $PM_{2.5}$ cutoff. $PM_{2.5}$ aerosol was sampled on the MARGA using a the new URG cyclone installed for this campaign (see Methods section 2.2.1), which was designed to match the instrument inlet flow rate of 16.7 lpm. During the dust events, the peak in mass loading occurs near the 2.5 μm cut point of the cyclone (Figure S7), suggesting that even small differences in the cut point of the ARA and MARGA inlets could lead to large differences in measured NO_3^- concentrations. Flows through the MARGA inlet were monitored continuously in the field, but subsequent testing of the $PM_{2.5}$ inlet suggests that approximately 20% of particles in the 3 to 5 μm size range and 10% of particles in the 5 to 10 μm size range transmit through the cyclone (Figure S8). The lower efficiency of the $PM_{2.5}$ cyclone may have been partially due to the pressure drop from deployment of a PM_{10} cyclone in series with the $PM_{2.5}$ cyclone. Alternatively, the ARA measurement could be under-measuring concentrations of $PM_{2.5}$ nitrate, due to less than 100% Nylon collection and extraction efficiencies; however, these losses are minor (less than 10%). Both of these

possibilities are consistent with the dust event uptake occurring predominately onto coarse-mode particles, which would be more efficiently detected by the MARGA rather than the ARA monitors. In addition, the E-AIM model output matches the ARA NO_3^- measurement more closely than that of the MARGA measurement (Figure 7d, main text). Because E-AIM omits explicit characterization of mineral cations, this result is consistent with the MARGA measuring dust-derived nitrate and the ARA system measuring predominately fine mode NH_4NO_3.

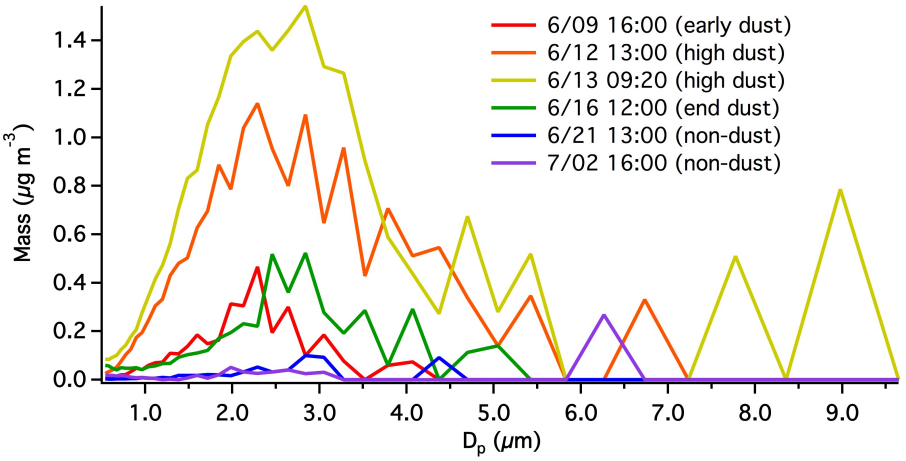

Figure S7: Mass distribution of aerosols of given diameters at times before, during, and after the second coarse particle event during the 2013 SOAS campaign. This distribution indicates peak mass loading occurred near 3 μm, indicating that small discrepancies in instrument inlet $PM_{2.5}$ size cut could lead to large differences in measured NO_3^- concentrations.

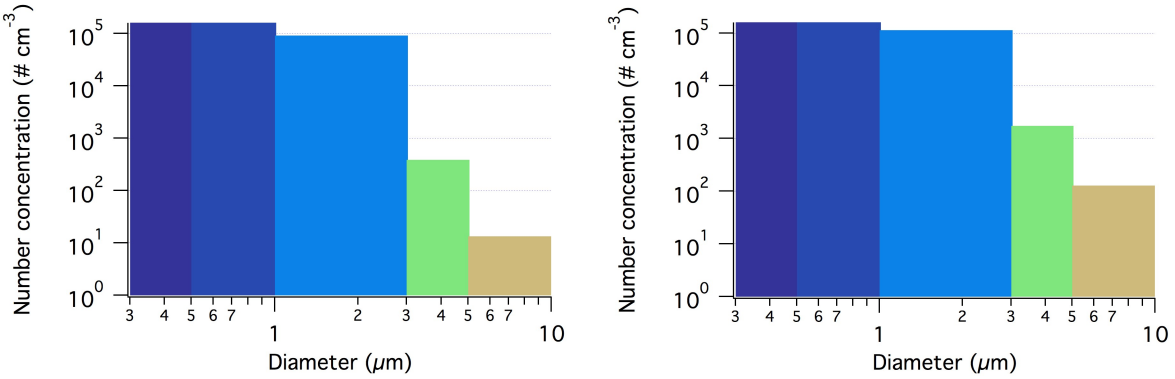

Figure S8: Number size distribution of Portland, OR particles (left) pulled through the $PM_{2.5}$ cyclone used with the MARGA inlet during the SOAS campaign at 16.7 lpm, and (right) without the cyclone, in both cases averaged for several interleaved 5 minute intervals during which particle size distribution was constant. Approximately 20% of particles in the 3 to 5 μm size range and 10% in the 5 to 10 μm size range transmit through the cyclone. During dust events at SOAS, the particle size distribution peaked near 3 μm, suggesting that slight differences in $PM_{2.5}$ size cuts of instrument inlets could have a substantial effect on measured aerosol concentrations.

Although differences exist between the three HNO_3 measurements and the two NO_3^- measurements, these discrepancies do not appear to substantially affect the predicted rate of HNO_3 heterogeneous uptake on crustal dust (see section 3.5). The rate derived from HNO_3 measurements made by the ARA instrument and by the CIMS are very similar to that derived from the MARGA HNO_3 measurements (Figure S9).

The rate of uptake is driven primarily by the availability of coarse particle surface area (section 3.5), and therefore discrepancies in measurements of HNO_3 do not greatly impact the average rate at which NO_3^- forms in the aerosol phase from this process.

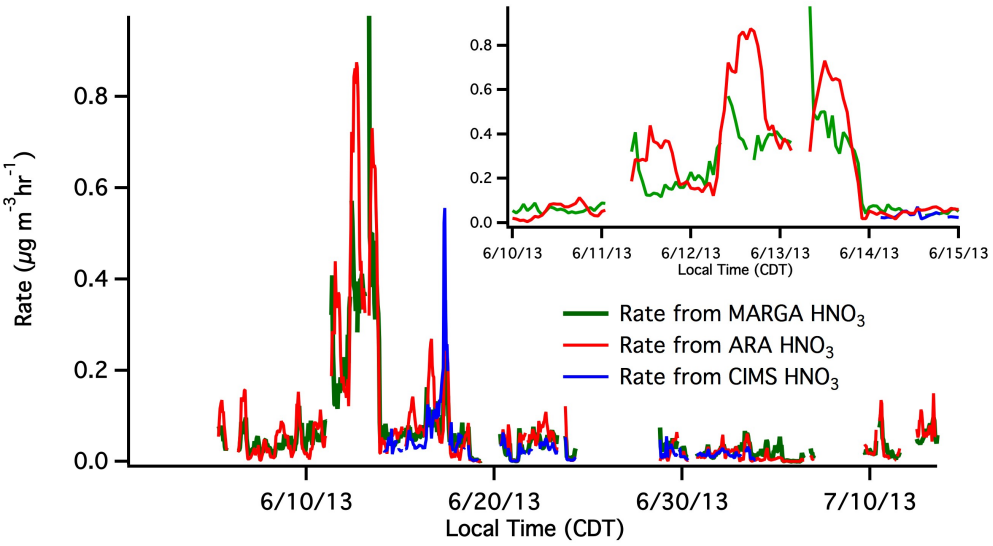

Figure S9: Comparison of the rate of HNO_3 uptake on crustal dust (see section 3.5) employing HNO_3 measurements made by MARGA, the ARA instrument, and by CIMS, with inset showing the predicted rate for the first coarse particle event. The discrepancies in measured HNO_3 do not appear to significantly alter the magnitude of the predicted uptake rate.

4 Historical data

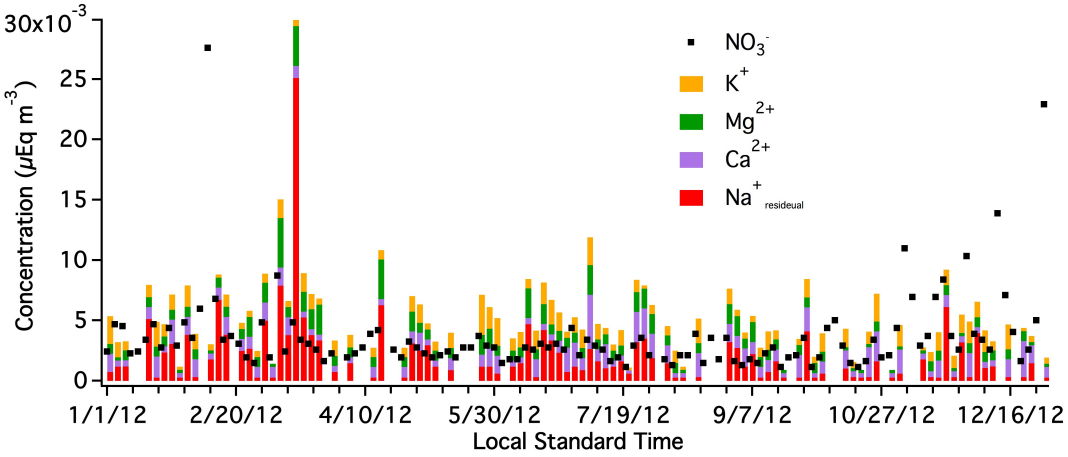

Figure S10: Time series showing concentrations of stacked K^+, Mg^{2+}, Ca^{2+}, and $Na^+_{residual}$ (Na^+ subtracting Cl^- equivalents) compared with NO_3^- for the year 2012 at the Centreville measurement site.

Data collected at the Centreville measurement site provides a historical context for analysis of nitrate and crustal dust interactions. Figure S10 gives a year-long look at concentrations of crustal minerals compared with aerosol NO_3^- and shows the direct correlation between the two. Table S1 shows values of acidity, defined as the slope of $[SO_4^{2-}]$ vs. $[NH_4^+]$ (in μEq m^{-3}) correlations for each year, along with the number of sea salt and crustal dust events that year. Sea salt events are defined as the number of points (3-day averages) of the ratio Cl^-/Na^+ at or above a value of 1.164. Crustal dust events are defined by the number of points (3-day averages) of nss-Na^++Ca^{2+} at or above a value of 0.1 μg m^{-3}. The sea salt and crustal dust events,

and their correlation with NO_3^- occur throughout the year, but most frequently during the spring and summer months when temperatures are warmer.

Table S1: Historical acidity, number of sea salt events, and number of crustal dust events for the Centreville measurement site from 2008-2012. The 2013 SOAS campaign had an acidity value of 1.12, similar to those of previous years.

Year	Acidity	Sea Salt Events	Mineral Events
2012	1.2	26	20
2011	1.08	20	24
2010	1.11	42	21
2009	1.16	37	12
2008*	1.12	28	14

Data collected using Teflon filters (ARA); *Note: 2008 begins April 19

References

DeCarlo, P. F. and Kimmel, J. R. and Trimborn, A. and Northway, M. J. and Jayne, J. T. and Aiken, A. C. and Gonin, M. and Fuhrer, K. and Horvath, T. and Docherty, K. S. and Worsnop, D. R. and Jimenez, J. L. (2006). "Field-deployable, high-resolution, time-of-flight aerosol mass spectrometer." *Anal. Chem.*, 78:8281-8289.

Edgerton, E. S. and Hartsell, B. E. and Saylor, R. D. and Jansen, J. J. and Hansen, D. A. and Hidy, G. M. (2005). "The Southeastern Aerosol Research and Characterization Study: Par II. Filter-based measurements of fine and coarse particulate matter mass and composition." *J. Air and Waste Manage. Assoc.*, 55:1527-1542.

Fry, J. L. and Draper, D. C. and Zarzana, K. J. and Campuzano-Jost, P. and Day, D. A. and Jimenez, J. L. and Brown, S. S. and Cohen, R. C. and Kaser, L. and Hansel, A. and Cappellin, L. and Karl, T. and Hodzic Roux, A. and Trunipseed, A. and Cantrell, C. and Lefer, B. L¿ and Grossberg, N. (2013). "Observations of gas- and aerosol-phase organic nitrates at BEACHON-RoMBAS 2011." *Atmos. Chem. Phys.*, 13:8585-8605.

Malm, W. C. and Sisler, J. F. and Huffman, D. and Eldred, R. A. and Cahill, T. A. (1994). "Spatial and seasonal trends in particle concentration and optical extinction in the United States." *J. Geophys. Res.*, 99:1347-1370.

Neuman, J. A. and Huey, L. G. and Ryerson, T. B. and Fahey, D. W. (1999). "Study of inlet materials for sampling atmospheric nitric acid." *Environ. Sci. Technol.*, 33:1133–1136.

Nguyen, T. B. and Crounse, J. D. and Teng, A. P. and St. Clair, J. M. and Paulot, F. and Wolfe, G. M. and Wennberg, P. O. (2014). "Rapid deposition of oxidized biogenic compounds to a temperate forest." *PNAS*, 112:E392-E401.